Bull Eng Geol Environ (2009) 68:107–116
DOI 10.1007/s10064-008-0180-z

ORIGINAL PAPER

Influence of the microstructure in the collapse of a residual clayey tropical soil

Nelcí Helena Maia Gutierrez · Maria Teresa de Nóbrega · Orencio Monje Vilar

Received: 20 February 2008 / Accepted: 24 August 2008 / Published online: 23 October 2008

Abstract A typical residual clayey soil originating from basalt in southern Brazil has been analyzed in order to assess the influence of wetting-induced deformation and microstructural features on the collapse behavior. Single and double oedometer tests were undertaken on a soil profile to 9 m depth. The results indicated collapsible behaviour at all profile depths. The influence of pre-consolidation stress and pedogenetic factors in the variability of the physical characteristics of the soil and in the magnitude of the collapse was noted. The collapse coefficient has been shown to be related to the both the microaggregate plasma and the varying nature of the pores and their interconnectivity.

Keywords Collapsible soils · Residual soils · Microstructure · Micromorphology

Résumé L'influence de la structure d'un sol ferrallitique, développé sur roche éruptive basique (basalte) du sud du Brésil, sur l'effondrement lors du mouillage a été étudiée à partir d'essais œdométriques et d'analyses micromorphologiques. Il a été établi des corrélations entre la dynamique d'effondrement et l'évolution de la macrostructure et de la microstructure du sol. Les essais œdométriques simples et doubles ont été réalisés sur des échantillons pris jusqu'à 9 m de profondeur. L'amplitude d'effondrement reste fortement dépendante de facteurs pédogénétiques et de la contrainte de pré-consolidation. Les valeurs les plus hautes du coefficient d'effondrement semblent êtres dues à la présence d'un plasma à l'échelle des microaggrégats, à la porosité intermicroaggrégats, et au degré de connectivité entre pores.

Mots clés Sols effondrables · Microstructure · Micromorphologie

N. H. M. Gutierrez (✉)
Departamento de Engenharia Civil, Universidade Estadual de Maringá, Av. Colombo, 5790, Jardim Universitário, Maringá, PR 87020-900, Brazil
e-mail: aamgutierrez@wnet.com.br

M. T. de Nóbrega
Departamento de Geografia, Universidade Estadual de Maringá, Av. Colombo, 5790, Jardim Universitário, Maringá, PR 87020-900, Brazil
e-mail: mtnobrega@uol.com.br

O. M. Vilar
Departamento de Geotecnia, Universidade de São Paulo, Escola de Engenharia de São Carlos, Av. Trabalhador São Carlense, 400, São Carlos, SP 13566-590, Brazil
e-mail: orencio@sc.usp.br

Introduction

All soils are deformed when subjected to loading. The type and magnitude of deformations and the time necessary for stabilization of the soil depend, among other factors, on the applied stress, moisture conditions and the inherent properties of each type of soil. However, some non-saturated soils experience an abrupt volume decrease when they are wetted, even if the total stress remains constant. This wetting-induced phenomenon is called collapse and the soils collapsible or metastable. Although some collapsible soils, when soaked, collapse under their own weight, more commonly collapse- or wetting-induced deformation is the result of a combination of loading followed by wetting (Dudley 1970).

Collapsible soils are found in various regions of the world (especially in tropical climates) and encompass a

great variety of geological materials. Some cases reported in the literature state that these soils are predominantly constituted of sands or silts. They are characterized by an open unstable structure and water contents less than necessary for saturation. Particles are maintained in their positions in the soil structure by means of bonds capable of providing temporary additional strength. This bond may be created by suction (capillary and adhesive forces) and/or such cementing substances as iron oxides and carbonates. As these forces tend to decrease or even vanish after wetting, shear failure and volume decrease may occur.

Several cases of collapsible clayey soils have been reported in Brazil, generally associated with volcanic rocks in the central and southern regions of the country, in the sedimentary basin of the state of Paraná. Although these clayey soils result from intense in situ geochemical and pedogenetic alterations of basalts, in some instances they may be associated with transported material, such as colluvium which has also been affected by the pedogenetic processes typical of hot and humid tropical conditions. These low saturation porous clayey soils are classified as oxisols (American classification) and as ferrasols (FAO-UNESCO) and usually extend to up 5 m, but they can sometimes extend to depths exceeding 10 m.

The microstructure is acknowledged to be a decisive factor in the characteristics and behaviour of soils (Mitchell 1956; Collins and McGown 1974), especially for those soils developed in a tropical environment. However, knowledge of the microstructure of tropical soils, where collapses have been more evident, is still scanty compared to that of soils in temperate regions (Collins 1985).

This paper presents test results from a clayey tropical soil derived from basalt in the northern region of the state of Paraná, Brazil. The collapse behavior of this soil at different depths was evaluated by varying the water content and load. Single and double oedometer tests (soaked at different stresses) were undertaken to determine the collapse and its magnitude. Observations by binocular magnifying glass and micromorphological analyses of thin sections cut vertically through undisturbed samples before and after collapse were used to analyze the modifications of the macro and microstructure and their influence on soil collapse.

Materials and methods

The samples were obtained from a basalt residual clayey soil (oxisol) in the city of Maringá, in the northern region of the state of Paraná, southern Brazil.

The field investigation comprised auger borings to establish the type of materials, vertical variations of the soil and the location of the ground water level as well as standard penetration tests and visual observation through an inspection hole. This large diameter (1 m) well, which extended to the weathered basalt at some 9 m depth, was used to obtain disturbed and undisturbed samples. Seven hand-carved undisturbed blocks (30 × 30 × 30 cm) were obtained at about 1.5 m spacings.

Samples from the well and 15 m deep auger boring were tested for particle size, liquid and plastic limit and unit weight. The laboratory tests also included double and single oedometer tests (flooded under controlled conditions). In the single oedometer tests, specimens were loaded at natural moisture content up to the following stresses: 12.5, 25, 50, 100, 200, 400 and 800 kPa. After equilibrium under these loads, the specimens were soaked and the additional deformations (collapse) were measured until complete stabilization. In the double oedometer tests, two specimens of each sample, with similar characteristics, were concurrently tested to a stress of 800 kPa, one at natural moisture content and the other soaked after applying a 1.25 kPa stress. Unloading of the specimen was undertaken in steps at the end of each test.

Examination of the acrylic resin-impregnated materials was undertaken using a binocular magnifying glass and micromorphological analyses of the thin sections (adapted from Verbeke 1969). The micromorphological analyses included undisturbed soil and samples tested in the oedometers before and after collapse. The criteria and terminology proposed by Brewer (1976) were adapted for the micromorphological description.

Results and discussion

Physical characterization of the materials of the soil profile

Figure 1 presents a typical soil profile, SPT *N* numbers from borings B1 to B3 and the results of the grain size, liquid and plastic limit and unit weight tests. The analyses of the field and laboratory data allowed the soil profile to be separated into two well-defined groups:

- The upper group, of reddish brown silty clay (oxisol) had SPT *N* values varying from 1 to 4 at the surface to 8 between 7.0 and 9.0 m depth. The unit weight varied from 29.8 to 30.8 kN/m^3. The liquid limit was between 57 and 73%; the higher values being near the base (at the transition to the lower group). The plasticity index ranged between 15 and 24%.
- The lower group, present from about 9 m depth, had a larger range of texture than the upper group and colour variation. It usually showed dyaclases with black and/or yellow oxidation. The SPT *N* values were higher

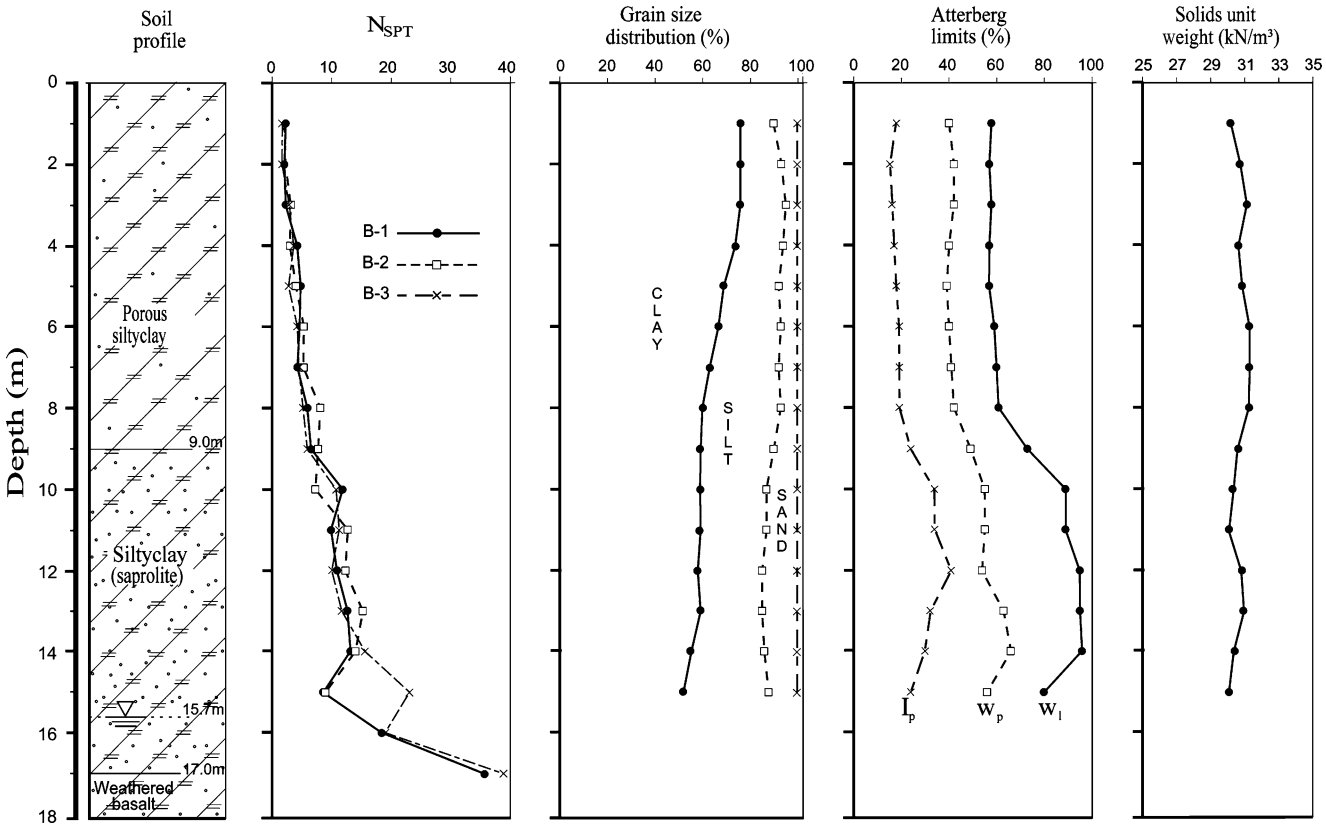

Fig. 1 Typical basalt residual soil profile (Maringá-Paraná, Brazil)

than those of the upper group, although with some variation at depth. The liquid limit was over 80%, reaching up to 96%. The plasticity index varied from 24 to 41%. The unit weight varied from 29.7 to 30.5 kN/m^3. This group corresponds to the completely weathered basalt horizon, retaining some features of the parent rock (basalt or basalt saprolite).

An interesting feature is that the upper group, although more clayey, had a lower plasticity than the lower group. This is partly explained by the difference in mineralogical composition of the clays and partly by the granular structure generated by the more active pedogenetic processes in the upper group, which might result in a locking of the clay fraction by iron oxides/hydroxides (Chauvel et al. 1976).

Beneath these two groups, at about 17 m depth, basalt was found with varying degrees of weathering, depending in part on whether the material was dense, vesicular and/or amygdaloidal. The ground water level was found at about 15.7 m depth, in the basalt alteration layer.

Table 1 shows the results of the characterization tests together with the physical indices of the soils as measured in specimens molded for the oedometer tests. The high soil void ratio—2.5 at 3.2 m depth—is of note; void ratios tend to decrease with depth, but are larger than 1.5 at 9.25 m. Another important observation, which is typical of residual soils, is the inherent variability of the physical properties. As shown in Table 1, the coefficient of variation of void ratio is higher than 2% at 9.25 m and reaches 8% at 3.2 m.

In this clayey soil, the water retention capacity is high and the natural moisture content is over 30% at all depths. However, high moisture contents do not imply high saturation levels, as the void ratios are relatively large. The degree of saturation is about 50% at the surface and increases with depth, reaching about 66% at 9.25 m depth. High void ratio and low saturation degree imply a low dry unit weight of the soil; values as low as 9 kN/m^3 have been reported in the upper levels.

Soil behavior and collapsibility

Figures 2 and 3 show compression curves from the single and double oedometer tests for sample 2 (1.6 m). The observed behavior may be regarded as typical of the most developed pedological materials that form the upper profile.

Figure 2 shows compression curves and wetting-induced deformation (collapse deformation) measured under overburden stresses of 12.5, 50, 200, 400 and 800 kPa. The void ratios are normalized relative to the initial void ratio. It can be seen that deformation is

Table 1 Characteristics of soil of the upper group and transition zone for lower group

Sample	1	2	3	4	5	6	7
Average depth (m)	0.50	1.60	3.20	4.70	6.25	7.80	9.25
γ (kN/m^3)	13.75–15.25	13.06–13.85	11.43–13.48	14.19–16.24	15.41–16.15	14.37–16.20	14.84–15.63
w (%)	32.5–32.8	31.1–32.4	30.8–32.3	30.1–30.6	29.5–30.7	31.3–31.9	35.4–36.0
γ_d (kN/m^3)	10.36–11.51	9.90–10.46	8.72–10.28	10.86–12.47	11.85–12.38	10.94–12.31	10.96–11.52
γ_s (kN/m^3)	29.8	30.3	30.7	30.3	30.8	30.8	30.2
e	1.590–1.877	1.897–2.062	1.986–2.523	1.429–1.789	1.488–1.598	1.502–1.814	1.622–1.756
$\bar{e}$[a]	1.764	1.968	2.205	1.610	1.545	1.632	1.674
Se[b]	0.113	0.049	0.177	0.110	0.037	0.081	0.034
S^{2}e (%)[c]	6.388	2.467	8.025	6.864	2.413	4.954	2.046
S_r (%)	52.0–61.1	46.9–51.8	37.9–49.1	51.8–63.9	57.2–63.0	53.2–64.8	60.9–66.5
w_l (%)	58	57	58	57	59	61	73
w_p (%)	40	42	42	39	40	42	49
I_p (%)	18	15	16	18	19	19	24
Clay (%)	76	76	76	69	67	60	59
Silt (%)	14	17	19	23	26	32	31
Sand (%)	10	7	5	8	7	8	10

[a] Average void ratio

[b] Standard deviation of void ratio

[c] Variation coefficient of void ratio

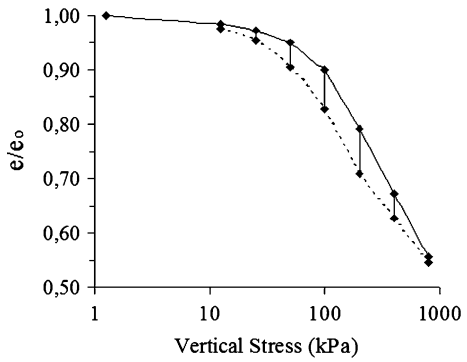

Fig. 2 Effect of soaking of specimen—single tests—sample 2 (depth 1.6 m)

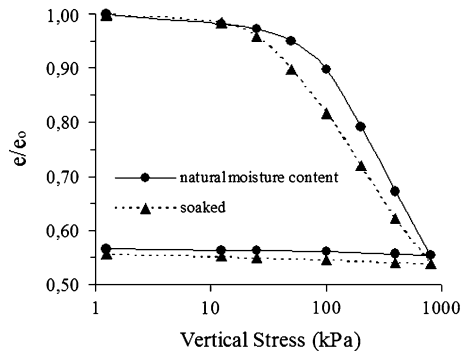

Fig. 3 Results obtained in the double oedometer test—sample 2 (depth 1.6 m)

negligible up to 12.5 kPa, reaches its maximum (6.4%) at 200 kPa and then decreases progressively to become negligible at 800 kPa.

Figure 3 shows the normalized confined compression curves in the natural and soaked conditions. As in the single oedometer tests, deformations are negligible with the lower stresses, reach a maximum of 6% at 100 kPa and thereafter decrease with increasing stress to less than 2% at 800 kPa.

Figure 4 illustrates total vertical overburden stress (σ_o), virtual pre-consolidation stress (σ_p) and soil compression indices in the natural and soaked conditions along the depth profile. It can be seen that the lowest pre-consolidation stress is associated with the sample from 3.2 m in the natural and soaked conditions. Between 4.5 and 9.25 m, the lowest pre-consolidation stresses were reported for material from 7.8 m depth.

The soil is overconsolidated at both natural moisture content and in the soaked conditions; as expected the larger overconsolidation ratio was observed for the samples tested at natural moisture content. The pre-consolidation stresses must be considered as virtual pre-consolidation stresses, as suggested by Vargas (1973), as they originated from different mechanisms than those that cause pre-consolidation in saturated soils of sedimentary origin, typical of temperate regions. Pre-consolidation stresses are reduced when the soil is soaked, but they are still higher than overburden stresses, except for the samples at 3.2 m depth. The

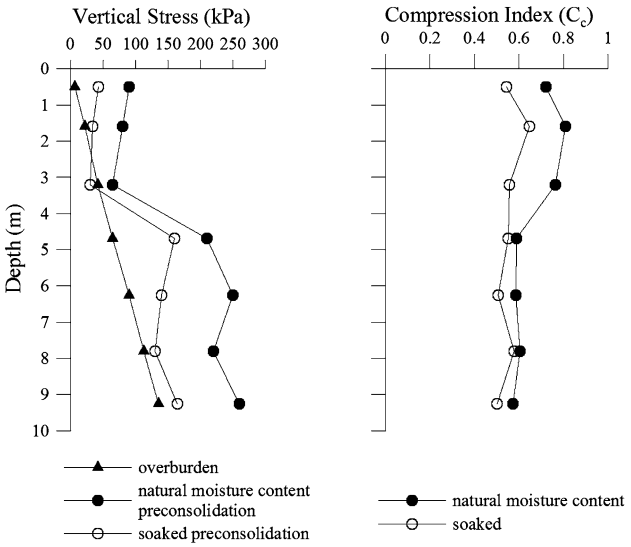

Fig. 4 Overburden and virtual pre-consolidation stress and compression indices of the soil at different depths

variation of pre-consolidation stress after soaking is a typical feature of collapsible soils in southern Brazil.

The greatest difference between virtual pre-consolidation stress and overburden stress (σ_p/σ_0) was found at up to 1.6 m depth. Amongst the many mechanisms that give rise to overconsolidated behavior, the wetting and drying cycles to which the soil was exposed since its formation are likely to be one of the most important. However, it should be noted that between 4.7 and 6.25 m depth, the difference increased again, probably due to the structural conditions at these levels (microaggregation reduction).

The compression indices also tend to decrease when the sample is soaked; the variation between the two conditions being greatest nearer the surface.

Figure 5 shows the coefficients of structural collapse obtained in the single oedometer tests in which the samples were soaked under known overburden stress. The coefficient of structural collapse has been calculated by:

$$I = \frac{\Delta e_c}{1 + e_i} \quad (1)$$

where Δe_c is wetting-induced variation of void ratio and e_i void ratio of soil before soaking.

The collapse coefficient values indicate that materials at different levels behave differently on wetting. Figure 5 shows that in all samples the coefficient of soil collapse tends to increase with the applied stress until it reaches the maximum value, after which it decreases to a minimum.

In the upper part of the soil profile (samples 1, 2 and 3), the highest collapse coefficients were between 4.8 and 6.4% for stresses between 50 and 200 kPa. At the deepest levels (samples 5, 6 and 7) the highest collapse coefficients

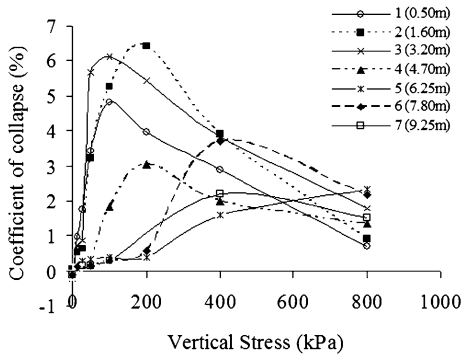

Fig. 5 Variation of coefficient of collapse in single oedometer tests

were between 2.2 and 3.7%, for stresses between 400 and 800 kPa. For sample 4, at the intermediate depth of 4.7 m, the highest coefficient was 3%, at a stress of 200 kPa. It is interesting to note that when sample 3 was soaked under 50 kPa stress (single test), close to vertical overburden stress (44 kPa), it showed a high coefficient of structural collapse (5.7%). In general, the larger collapse deformations are associated with the largest void ratios (samples 1, 2 and 3) and at lower stresses.

Figure 6 shows variations of the coefficient of collapse throughout the depth range for different applied stresses in the single tests. That same trend was also observed for the double tests and shows that the materials closer to the surface (up to approximately 4.5 m depth) have a different behavior from that of the materials at deeper levels.

If 2% of collapse deformation is assumed as the boundary between collapsible and non-collapsible soil, it may be seen from Fig. 6 that in this soil collapse is important up to a depth 4.5 m, for stresses between 50 and 400 kPa.

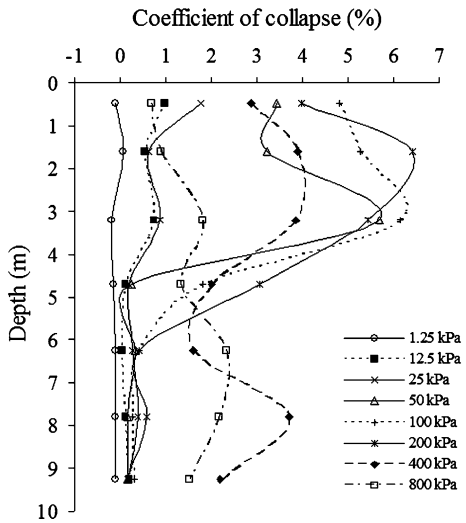

Fig. 6 Variations of coefficient of collapse along the depth—single tests

Figure 7 relates the coefficient of collapse with the ratio between the stress acting during soil soaking (σ_i) and virtual pre-consolidation stress (σ_{pn}) for the soil at its natural moisture content. It can be seen that the highest coefficients of structural collapse are associated with a relationship between soaking stress and natural preconsolidation stress (σ_i/σ_{pn}) of 1.0 and 3.2. The highest relationships, 2.5 and 3.2, were obtained for samples 2 and 5, from 1.6 to 6.25 m, respectively. The maximum collapse deformation (approximately 6%) occurs when σ_i/σ_{pn} is between 1.5 and 2.5.

Reginatto and Ferrero (1973) have proposed the following relationship to identify collapsible soils:

$$C = \frac{\sigma_{ps} - \sigma_o}{\sigma_{pn} - \sigma_o} \quad (2)$$

where C is coefficient of collapsibility, σ_o overburden stress, σ_{pn} pre-consolidation or yield stress (natural moisture content) and σ_{ps} pre-consolidation or yield stress (soaked specimen).

Soils have been classified as "truly collapsible" when $C < 0$, i.e., the soil collapses without any external loading. Soils have been classified "collapsible" when C is between 0 and 1, i.e., collapse depends on the stress level induced by external loading. Using this classification, Fig. 8 shows the coefficient C for the samples tested.

Mineralogy and micromorphology of the soil's constituent materials

The X-ray diffraction mineralogical analyses undertaken on oxisol powder obtained from sample 2 (1.6 m depth) indicate that it is composed predominantly of kaolinite, gibbsite, hematite and small quantities of quartz.

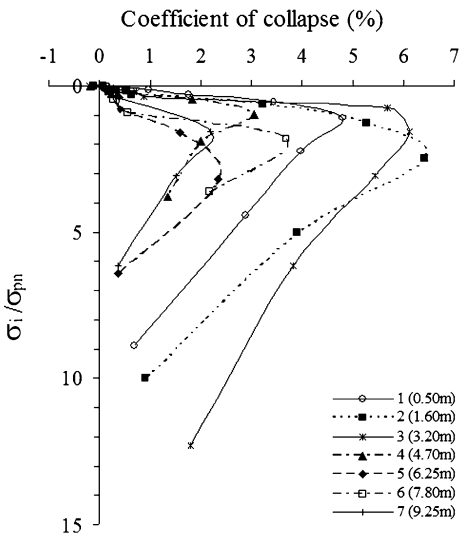

Fig. 7 Coefficient of collapse with the ratio between the stress acting during soil soaking and virtual pre-consolidation stress for the soil at its natural moisture content

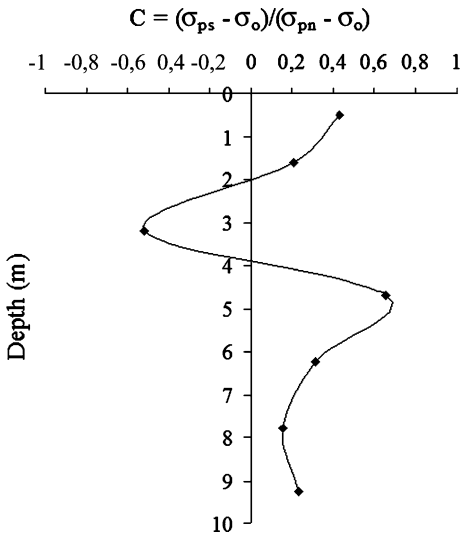

Fig. 8 Coefficients of collapsibility according to Reginatto and Ferrero (1973)

Micromorphological observations by the binocular magnifying glass and thin section optical microscope show (Fig. 9a) the material is mainly microaggregates (M), ranging from rounded to sub-rounded, whose arrangement (packing) produces a high inter-microaggregate porosity (high compound packing voids). Microaggregates are essentially formed by plasma (clay fraction <2 μm) ferric-clay, of a dark red color, with narrow bands of lighter red plasma (yellow or orange, in polarized light) at the borders, occasionally including grains of the skeleton (sand fraction) consisting of dark minerals (ilmenite, magnetite) and quartz (Q). The largest microaggregates ranged from approximately 200 to 400 μm, although the rounded material could reach 700 μm.

Oval or circular cavities—CV (section of tubes or channels) are frequently found in the microaggregate plasmas areas and are the result of biological activity (Fig. 9b). As a rule the oval cavities are larger: ranging from 4,000 to 2,000 μm. Some cavities are partially filled by microaggregates which are smaller than those of the surrounding area and probably related to root development.

Microaggregate zones increase towards more continuous plasma zones, as shown in Fig. 10a, where irregularly shaped microcavities may be present. As a rule, no large pores are found in these continuous plasmas zones and angular irregular grains of dark minerals and quartz (fine sand) up to approximately 50 μm are more common. Elsewhere, the microaggregates appear to be bonded by the lighter red plasma. Parallel and curved microfissures develop in the continuous plasma zones, probably produced by the wetting and drying of the soil in the surface layers (Fig. 10b).

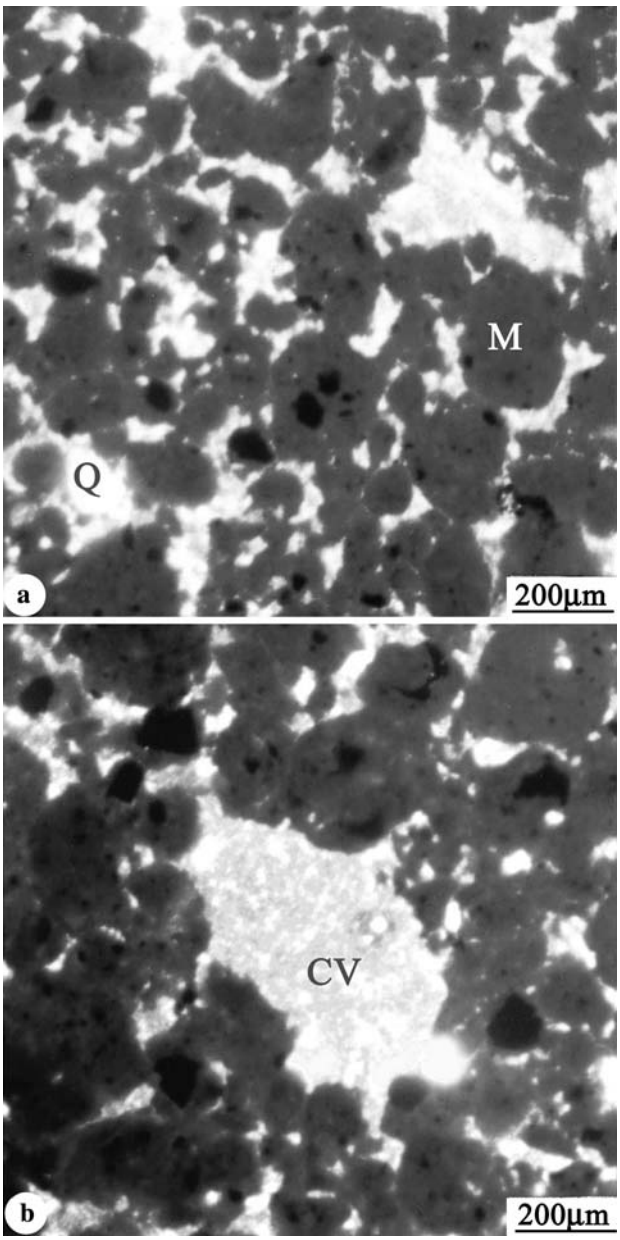

Fig. 9 Natural material (sample 2–1.6 m) observed by optical microscope with polarized light: **a** microaggregate zone, **b** microaggregate zone with oval cavity

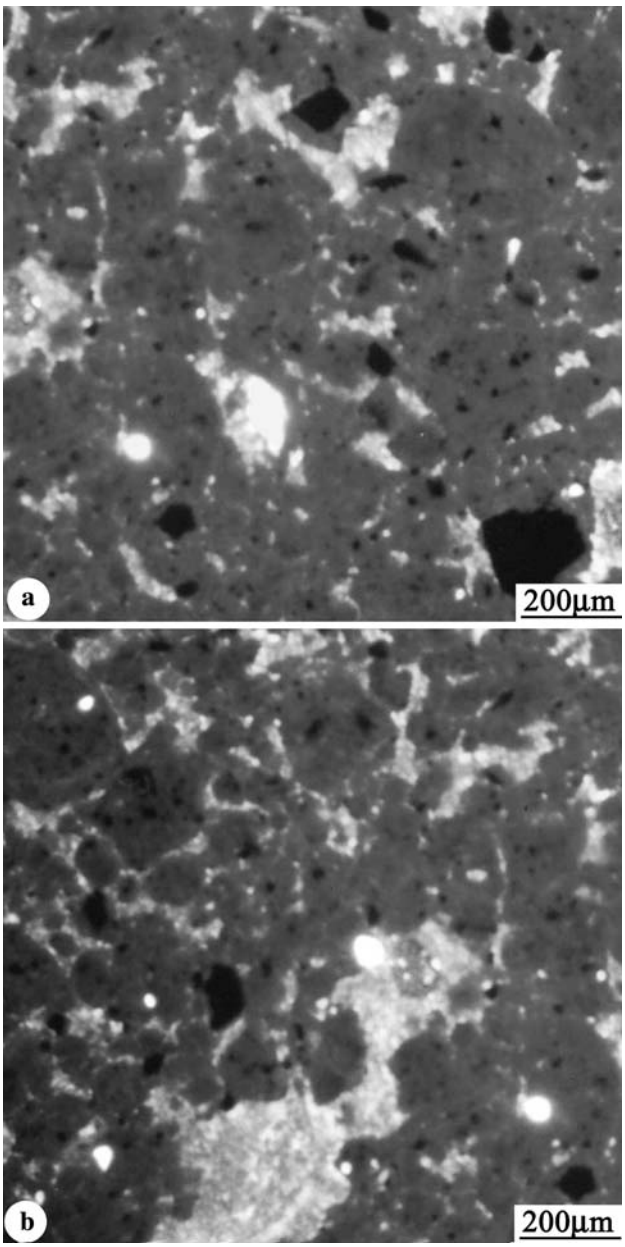

Fig. 10 Natural material (sample 2–1.6 m) observed by optical microscope with polarized light: **a** passage of the microaggregate zone to the continuous zone, **b** coalescence of microaggregates

From the binocular and optical microscopy examinations, it was seen that in pre-collapse conditions (loading up to 200 kPa, without soaking of the specimen), the macropores (higher than 2,000 µm) in sample 2 (1.6 m) were deformed from an oval to an irregular shape. Pores smaller than 1,000 µm generally kept together, were not deformed and had a more closed porosity (Fig. 11a). This is consistent with the total porosity, e.g., in an undisturbed sample the total porosity was 66% before and 65% after loading.

Figure 11b shows that after collapse (loading up to 200 kPa, with soaking) there is a significant reduction in inter-microaggregate porosity, reaching 58%. In this context, deformation affects mainly the pores, which in some cases undergo occlusion. Long, narrow and curved pores occur. Continuous plasma zones predominate, with zones with strong microaggregate coalescence such that the pores lose their connectivity and have a cavity-type porosity. There is evidence of compression of borders (orientation of plasma) and the appearance of parallel or perpendicular curved rifts (prolonged voids) within the microaggregates'

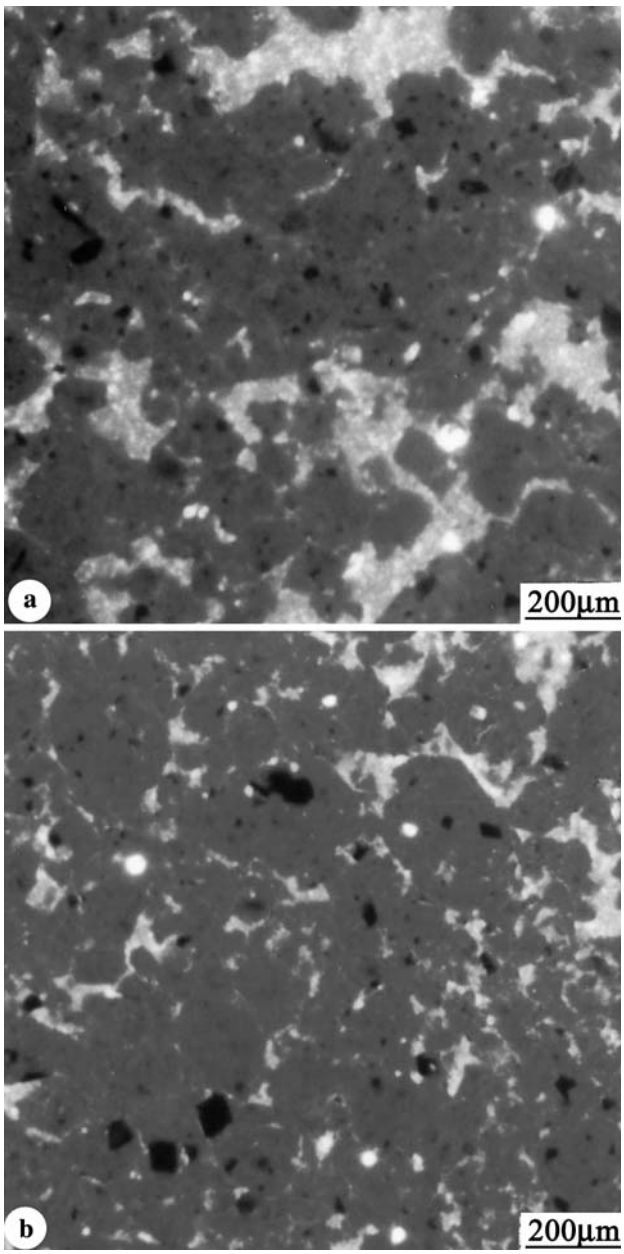

Fig. 11 Sample 2–1.6 m loaded up to 200 kPa, observed by optical microscope with polarized light: **a** without soaking (before collapse), **b** after soaking (after collapse)

contact zones. In some areas, microaggregates do not change, implying that the water ingress was not homogeneous.

Figure 12 shows material after collapse at a stress of 200 kPa and reloading up to 400 kPa. It has a predominantly continuous aspect, with high porosity zones formed by cavity or interaggregate, weakly communicant pores. There is a trend for the lengthening of pores and their distribution along parallel lines (stretching of pores). Irregularly shaped macropores are present and the plasma is more homogeneous in color: the greater welding of

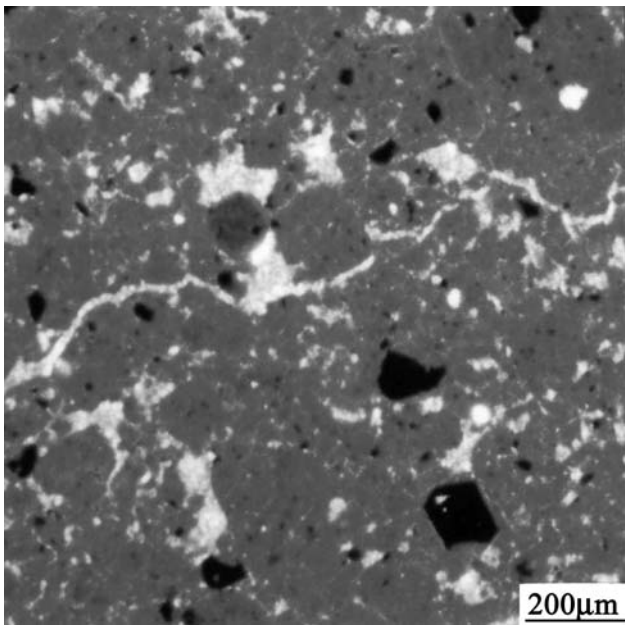

Fig. 12 Sample 2–1.6 m after collapse and reloading, observed by optical microscope

microaggregates reducing the yellowier strips of the borders. A general porosity of 54% has been reported, the degree of intercommunication varying. Plasma orientation around skeleton grains is more evident and more abundant. Fissures are short, curves are irregular and discontinuous, more frequent and generally follow the microaggregate borders. In some areas the structure still appears to be continuous microaggregate, welded and maintaining an important, albeit cavity-type, porosity.

The microscopic studies on the undisturbed samples indicate that there is a change in the relative proportions between microaggregate plasma and continuous plasma below approximately 4.5 m. Continuous plasma appears more frequently, intermixed with microaggregate zones. This variation in the plasma organization is reflected in the variation in porosity and type of pores (Fig. 13a). The transition is never sudden, as a consequence of the different evolutionary stages involved. Initially the continuous plasma is divided by short, fine fissures (fissure and cavity porosity), which develops into interconnected microaggregate zones. The total porosity of the material reaches 61%, somewhat less than most samples at the surface.

In areas of microaggregate plasma, the larger microaggregates are rounded and the smaller ones more irregular. As recorded for surface levels, they are formed by dark red plasma bordered by a strip of yellowish red plasma (Fig. 13b). The light-colored plasma bridges towards the other microagregates and is generally more abundant at this level than in the upper zones. In the undisturbed samples

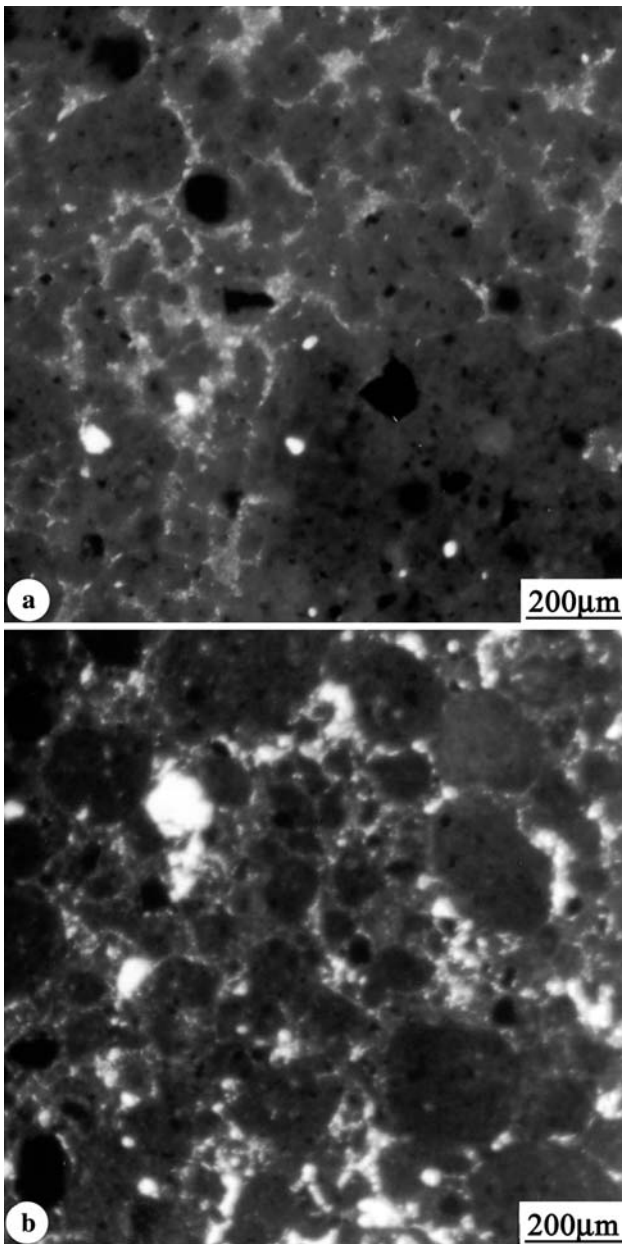

Fig. 13 Natural material sample 04–4.7 m observed by optical microscope with polarized light: **a** continuous and microaggregate zone, **b** rounded volumes formed by darker red plasma bordered by yellowish red plasma

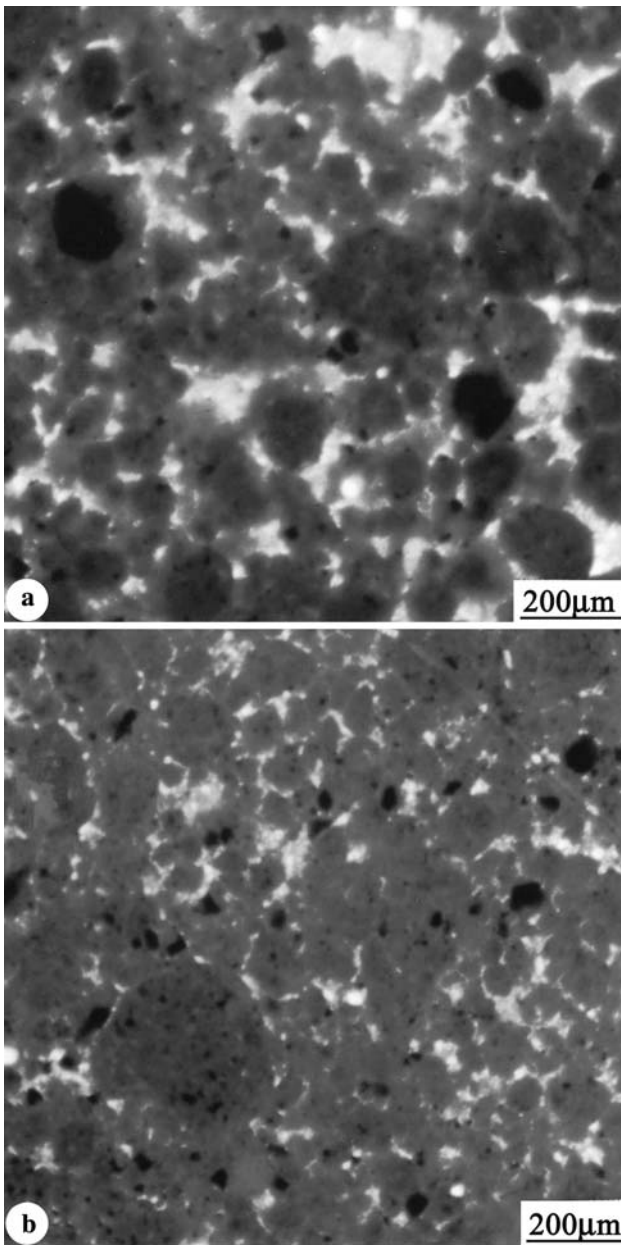

Fig. 14 Sample 4–4.7 m loaded progressively up to 200 kPa observed by optical microscope: **a** without soaking (before collapse), **b** after soaking (after collapse)

from approximately 4.5 m, the microaggregate borders are wider (yellowish) with different amounts of iron.

Figure 14a shows that, at a stress of 200 kPa (without soaking), there is practically no modification in the organization when compared to the unloaded sample, although a slight closing of the macroporosity is noted. The total porosity of the material is 60% and the orientation of the plasma around the larger grains is more striated that in the upper levels. There is also a greater deformation of the plasma borders (lighter part), with the more stable central part (darker) behaving as grains.

When loaded up to 200 kPa and soaked (after collapse), the thin section analyses indicated a reduction of microaggregate zones with interconnected compound packing voids (Fig. 14b). The porosity of 59% was largely related to individual cavities. Although there was some interconnection. Some zones are compressed and in other the microaggregate plasma is preserved. In areas of continuous plasma, the fissures are open with striated plasma at the edges. The lighter plasma is not always present and in some zones there is a tendency to void alignment, preferentially at some 45° to the vertical.

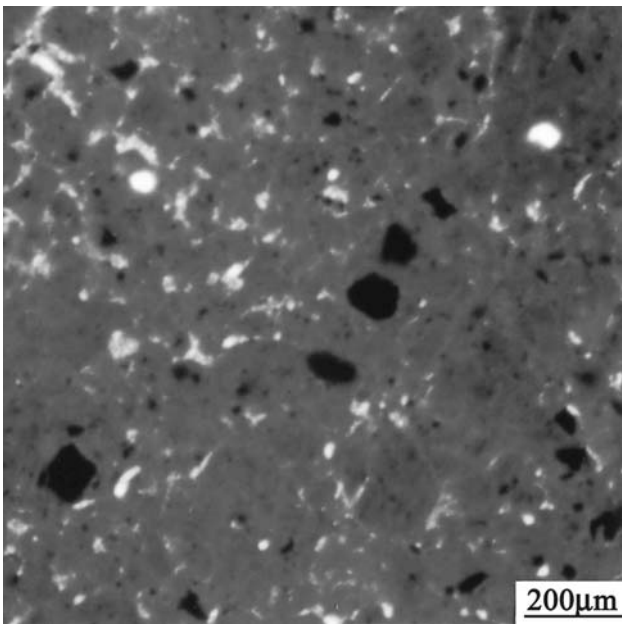

Fig. 15 Sample 4–4.7 m after collapse and reloading observed by optical microscope

For post-collapse and reloading up to 800 kPa analyses show (Fig. 15) that the structure is practically continuous, although some microaggregate zones remain. Extensive closing of porosity occurs (51%), essentially cavity-type with narrow and elongated pores. In the microaggregate zones, the initially rounded microaggregates lose their shape and become squarer with few sharp borders as they compress into each other. In the continuous zones, large deformations of the microaggregates are seen, with extensive plasma orientation.

Conclusions

The paper reports analysis of a clayey soil profile (oxisol) formed from basalt under tropical conditions. Oedometer tests have shown the soil's sensitivity to soaking. The upper part (above 4.5 m depth) was more liable to collapse than the deep material towards the interface with the saprolite at c. 9 m. A strong relationship between collapse coefficient and virtual pre-consolidation stress exists, probably related to the higher void ratios towards the surface and the microstructure of the material.

Microscopic analyses revealed changes in the plasma organization from 4.5 m depth, which may explain the changes in the material behavior on loading/soaking. In the upper part of the profile, a microaggregate plasma predominates, with an interconnected porosity and macrocavities of biological origin. These characteristics facilitate collapse.

Continuous plasma zones and microaggregate coalescence zones become more frequent below 4.5 m. These zones are associated with a reduction in interconnecting porosity and less tendency to collapse.

The study indicated the influence of microstructure in the relation between virtual pre-consolidation stress and overburden stress (σ_p/σ_0); the highest values found occurred up to a depth 1.6 m. It is considered that the wetting and drying cycles to which the soil was exposed during its formation are very significant. These relations also increase between 4.5 and 6 m depth, which is probably due to microaggregation reduction.

References

Brewer R (1976) Fabric and mineral analysis of soils, 2nd edn. Wiley, New York, p 482

Chauvel A, Pedro G, Tessier D (1976) Rôle du fer dans l'organisation des matériaux kaoliniques. Sci du Sol 2:101–113

Collins K (1985) Towards characterization of tropical soil microstructure. In: International conference on geomechanics in tropical lateritic and saprolitic soils, proceedings, vol 1. ABMS, Brasilia, pp 85–96

Collins K, Mcgown A (1974) The form and function of micro fabric features in a variety of natural soils. Géotechnique 24(2):223–254

Dudley JH (1970) Review of collapsing soils. J Soil Mech Found Div ASCE 96(3):925–947

Mitchell JK (1956) The fabric of natural clays and its relation to engineering properties. In: Proceedings of the highway research board, vol 35, p 693

Reginatto AR, Ferrero JC (1973) Collapse potencial of soils and soil-water chemistry. In: Proceedings of 8th international conference on soil mechanics and foundation engineering, vol 2. Moscow, pp 177–183

Vargas M (1973) Structurally unstable soils in southern Brazil. In: International conference on soil mechanics and foundation engineering, vol 2. Moscow, pp 239–246

Verbeke R (1969) Sur un procédé de fabrication de lames minces dans roches peu cimentées et des sols. Bull de la Soc Géol France Tomo 11(3):426–433